We are IntechOpen, the world's leading publisher of Open Access books Built by scientists, for scientists

4,800
Open access books available

122,000
International authors and editors

135M
Downloads

Our authors are among the

154
Countries delivered to

TOP 1%
most cited scientists

12.2%
Contributors from top 500 universities

CLARIVATE ANALYTICS BOOK CITATION INDEX INDEXED

WEB OF SCIENCE™

Selection of our books indexed in the Book Citation Index in Web of Science™ Core Collection (BKCI)

Interested in publishing with us?
Contact book.department@intechopen.com

Numbers displayed above are based on latest data collected.
For more information visit www.intechopen.com

Chapter 4

Loads Simulator System for Testing and Qualification of Flight Actuators

Nasim Ullah

Additional information is available at the end of the chapter

http://dx.doi.org/10.5772/62710

Abstract

The flight actuation system plays important role in the accurate guidance of the flight vehicles. The actuators driving the control surfaces are aerodynamically loaded during flight. The design, testing and selection process of the flight actuators play important role to ensure the stable and safe flight. Since a reliable flight actuation system can ensure appropriate guidance, the importance of qualification process cannot be neglected. Qualification of the actuators through field trials is a very costly and time-consuming process. The testing process using real flights takes more time and is costly. For ground testing, aerodynamic loading systems are used. The aerodynamic loading system is ground-based hardware in the loop (HWIL) simulator that can be used for exerting aerodynamic loads on actuation system of flight vehicles in real-time experiment. The actuation system under test is directly connected to the loading motor through a stiff shaft and the aerodynamics loading is applied in real time according to the flight trajectory generated by a flight computer.

This chapter is preliminarily focused on the basic working principle, mathematical modelling and torque/force control system design of the load simulator system. As a case study, the response and dynamics of the electrical aerodynamic loading system are analysed using mathematical modelling concept. The dynamic model is discussed and adaptive fuzzy sliding mode control techniques are introduced to ensure the high-performance torque loop of the aerodynamic loading systems.

Keywords: Ground-based testing, aerodynamic load simulators, flight actuators, mathematical modelling, modern control

1. Introduction

In a flight control system, aerodynamic loads are introduced during flight at the control surfaces or fins of flight vehicle as a function of air density, fin angle, etc. The fin control system must respond to these loads to maintain the accuracy of flight control system [1–3]. Since load simulators are used for the qualification of flight actuation system, the control performance of load simulators is vital [4, 5]. Before the invention of the motorized load simulators, the mechanical springs or torsion bars were utilized for the testing process. Conventional testing has several disadvantages, for example, the loading devices are not adaptable to varying loads. In modern ages, the testing and qualification of flight actuators are done through a hardware in the loop simulator system. In order to reduce cost and time, hardware in the loop simulators are utilized in which a loading motor is used as the aerodynamic loading device [6–9]. There are three types of load simulators depending on the type of applications and loading requirements [2–6]. Electro-hydraulic load simulators (EHLS) are widely used as hardware-in-the-loop-simulation (HILS) system in flight control applications that can simulate the air load executed on flight actuation systems. The EHLS can simulate rapid and large torque/force loads with big volume. Some advantages and disadvantages are listed. The hydraulic load simulators move fast and have rapid steering. The natural frequency of the electro-hydraulic servo valve is generally above 100 HZ, so the hydraulic load simulator's frequency response is very fast and smooth. The low-speed performance of electro-hydraulic actuator is good. The load simulators can be operated in wide speed range. On other hand, due to big size and volume, maintenance cost is high. Temperature effects can cause degradation of performance. At low temperature the friction loss is high, and at high temperatures the leakage phenomenon is significant. Leakage of hydraulic fluid or oil is a major drawback. It causes the environmental pollution. This can easily cause a fire. The oil contamination causes system blockage and system failures. Another type is the pneumatic load simulator that is a typical hardware in loop (HIL) system used to apply medium-range torque/force loads on the actuator under test. The pneumatic load simulator can track the fast deployed load with compressibility. Pneumatic systems are often used instead because pneumatic pressure is usually cheaper to obtain, especially since most industrial facilities already have compressed air available. The pneumatic load simulators use air or any other compressed gas to transmit power. It is hard to obtain smooth performance due to large compressibility factor, especially at low speeds. Similarly, temperature changes can degrade the performance of pneumatic load simulators. The pneumatic load simulators are smaller in size and volume as compared to hydraulic load simulators, so the maintenance cost is lower. The electrical load simulator is an important ground-based hardware tester simulator used for qualification of flight actuation system, such as the aircraft control surfaces, ship steering system, robotics arm, undercarriage of the plane and high-speed elevator system. The electrical load simulators are used to apply medium and small loads on actuators under test. Some advantages of electrical load simulator are its small size and volume, low installation and maintenance cost, less sensitive to temperature changes as compared to hydraulic and pneumatic load simulators and high performance. There are no environmental hazards associated with electrical load simulators.

http://dx.doi.org/10.5772/62710

2. Working of load simulator system

Laboratory testing and qualification of flight actuators play vital role for ensuring the design of reliable flight control with cost-effective solutions. The hardware diagram given in **Figure 1** is the minimal setup that is used in the laboratory testing of the flight actuators. The flight actuator is directly connected to the loading motor through a stiff shaft. The direct mechanical connection allows the application of the loading torque generated at the output shaft of loading motor in a close loop system. The Autopilot controller is used to set the reference position trajectory of the flight actuator. An important block of the system is the aerodynamic load calculator system, and the inputs to this block are the reference position command of the actuator system, air speed, Mach number and angle of attack. The output of the load calculator block serves as reference command to the loading motor. Thus, the torque load loop is closed using the feedback signal from torque sensor. The advantage of using the proposed setup provides the designer a freedom for applying real-time loads simulated in the laboratory with minimum cost.

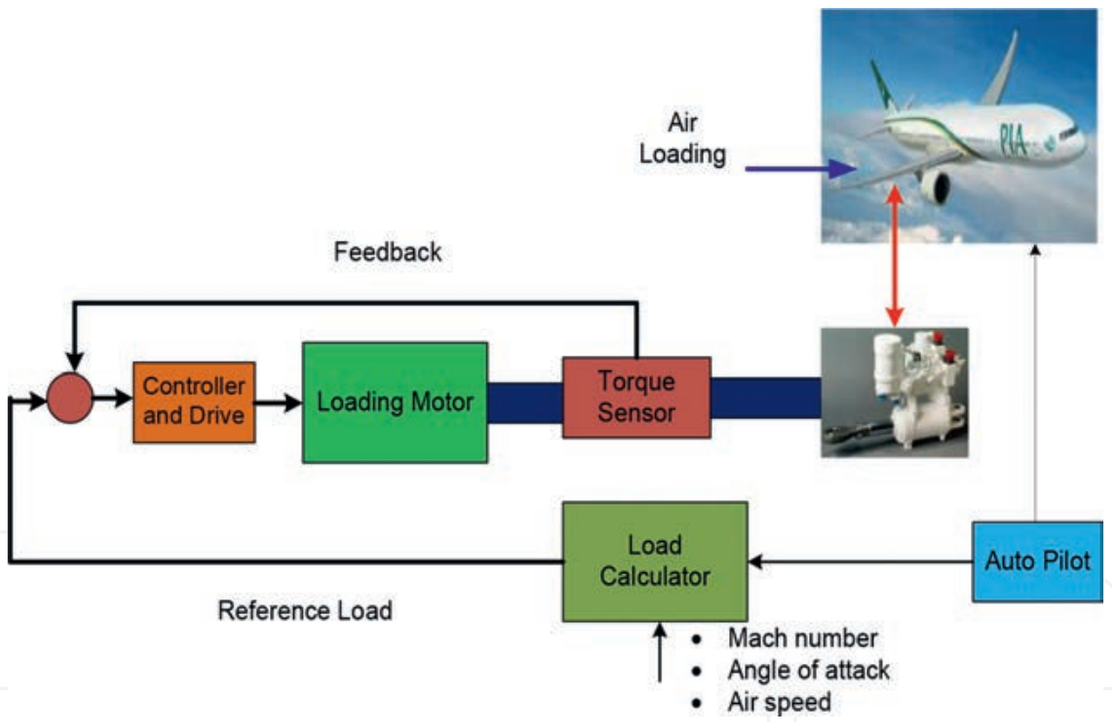

Figure 1. Block diagram of electrical load simulator.

3. Actuator testing: a case study

The flight actuator under test is a brushless DC motor. A permanent magnet synchronous motor (PMSM) is used as the loading motor. For simplicity, the load calculator is used in proportional mode. In proportional mode, the output of the load calculator is directly pro-

portional to the reference command of the flight actuator. Let θ_a represents the reference command of flight actuator, then the output of the load calculator T_r is $C\theta_a$ where "C" represents the proportionality constant. The parameter T_r is set as reference command of the torque loading motor. From **Figure 2**, the reference command signal of the flight actuator $\theta_a$is constructed from a real test scenario of a flight vehicle.

Figure 2. Reference signal command of flight actuator.

Before discussing the control problem, basic understandings of system dynamics is a pre requisite. A PMSM is used as a loading motor. The voltage and torque balance equations of PMSM loading motor are written as

$$\begin{aligned} u_d &= i_d R_s + L_{sd}\frac{di_d}{dt} - PL_s i_q w_m \\ u_q &= i_q R_s + L_{sq}\frac{di_q}{dt} + PL_{sq} i_d w_m + P\psi_m w_m \\ T_e &= \frac{3P}{2}[\psi_m i_q + \left(L_{sd} - L_{sq}\right) i_d i_q = J\frac{dw_m}{dt} + Bw_m + T_f + T_L \end{aligned} \tag{1}$$

In Eq. (1) $[i_d\, i_q]$ is the d-axis and q-axis current vector, $[u_d\, u_q]$ represents d-axis and q-axis voltage vector, w_m is the angular velocity of torque motor, $[L_{sq}\ L_{sd}\ R_s]$ represents inductances and resistances of ELS motor,$[P\ ,\ \psi_m]$ represents the number of pole pairs and magnetic flux of rotor, $[J,\ B]$ represents inertia and damping coefficient, $k_t = \frac{3P}{2}\psi_m$is torque constant, $k_b = P\psi_m$ is back emf constant, and $[T_e\ ,\ T_f,\ T_L]$ is the electromagnetic torque, friction torque and output load torque. Assuming that inertia and damping coefficient of torque sensor is very small, thus the dynamics can be written as

$$T_L = K_s\left(\theta_m - \theta_a\right) \tag{2}$$

Here, $[\theta_m\, \theta_a]$ represents the angular position of loading motor and actuator, K_s is the total stiffness of torque sensor and connecting shaft. To achieve largest torque operation and to

http://dx.doi.org/10.5772/62710

eliminate coupling effect between speed and currents, we set d-axis reference current $i_d^{'}$ equal to zero. Considering the effect of PWM driver and the current feedback, Eq. (2) can be written as given in [4]. For simplicity, we set $L_{sq} = L$ and $R_s = R$

$$\frac{di_q}{dt} = -\frac{R}{L} i_q - \frac{K_b}{L} w_m + \frac{K_v K_i}{L} \tag{3}$$

Here, k_i is the current controller gain. Current feedback is assumed to be unity. Assuming that load and friction torque are zero and taking Laplace transform of Eq. (3) and eliminating $I_{(s)}$, we get the transfer function from input voltage to output position as

$$\frac{\theta_m}{u_q} = \frac{\frac{K_v K_i}{K_b}}{S\left(t_m t_e S^2 + t_m S + 1\right)} \tag{4}$$

In Eq. (4), $t_m = \frac{RJ}{k_t k_b}$ is the electromechanical time constant, $t_e = \frac{L}{R}$ is the electromagnetic time constant. Replace Eq. (2) into Eq. (2), the simplified relation can be written as

$$\begin{aligned} T_L &= \frac{k_v k_i k_t u - s[(Ls+R)(Js+B) + k_b k_t] K_s \theta_a}{D(s)} \\ D(s) &= s\left[\left(Ls+R\right)\left(Js+B\right) + K_b K_t\right] + T\left(Ls+R\right) \end{aligned} \tag{5}$$

From the numerator of Eq. (5), it is concluded that extra torque is caused by the effect ofθ_a, θ_a and $\ddot{\theta}_a$. If the reference input command of loading torque motor is zero, i.e.$u = 0$, then Eq. (5) is reduced to the following simplified relation

$$T_L = \frac{-s[(Ls+R)(Js+B) + k_b k_t] K_s \theta_a}{D(s)} \tag{6}$$

From Eq. (6), it is concluded that extra torque is acting on the loading torque motor even if the reference input command u is zero. Extra torque is a function of the acceleration and velocity components of the actuators movement. After some simplifications, the state equation representation of electrical load simulator is written as

$$\ddot{T}_L = -a\dot{T}_L + bu - cf\left(T_{extra}, T_f, T_L\right) \tag{7}$$

In Eq. (7) the parameters are defined as

$$a = \frac{k_t k_b}{JR} + \frac{B}{J}$$
$$b = \frac{K_s k_t}{JR}$$
$$c = \frac{K_s}{J}$$
$$f\left(T_{extra}, T_f\right) = \frac{K_s}{J}\left(T_{sft} + T_f\right)$$

In Eq. (7) the nonlinear friction is represented using LuGre model, which is written as

$$T_f = a_0 Z + a_1 \dot{Z} + a_2$$
$$\dot{Z} = v - \frac{a_0 |v|}{g(v)} \tag{8}$$
$$g(v) = f_c + (f_c - f_s) e^{[\frac{v}{v_s}]^2} v$$

In Eq. (8) the parameter $g(v)$ is the Stribeck effect, v_s is the Stribeck velocity, f_c is coulomb friction, f_s is static friction, z is the average bristle defection, a_0 is the stiffness of the bristles, a_1 is the damping term and a_2 is the viscous friction coefficient. Now to realistically apply the loading torque on flight actuator, a feedback torque control system plays vital role. In this study, adaptive fuzzy sliding mode control system is used to formulate the torque control system.

3.1. Adaptive fuzzy sliding mode control for electrical load simulator system

Sliding mode is a robust control method which has been widely applied to many nonlinear systems [10–15]. This section provides an overview of derivations of torque control system for electrical load simulator's system. Let T_L be the output load torque and T_r be the desired torque signal, we define tracking error vector as

$$\begin{bmatrix} e = T_L - T_r \\ \dot{e} = \dot{T}_L - \dot{T}_r \\ \ddot{e} = \ddot{T}_L - \ddot{T}_r \end{bmatrix} \tag{9}$$

http://dx.doi.org/10.5772/62710

Error surface vector is defined as

$$\begin{bmatrix} s = \dot{e} + \lambda e \\ \dot{s} = \ddot{e} + \lambda \dot{e} \end{bmatrix} \tag{10}$$

Assuming that the nominal parameters of the system are known, then by combining Eqs. (7), (9) and (10) yields

$$\dot{s} = \left(-a\dot{T}_L + bu - f\left(T_{extra}, T_f\right)\right) - \ddot{T}_r + \lambda \dot{e} \tag{11}$$

The control law is given by

$$u = \frac{1}{b}\left(a\dot{T}_L + \hat{f}\left(T_{extra}, T_f | \theta\right) + \ddot{T}_r - \lambda \dot{e}\right) - \frac{1}{b}\left(K_d.s - w.sgn(s)\right) \tag{12}$$

From Eq. (12), it can be analyzed that the total control effort u is the sum of three terms

$$u = u_T + u_f + u_{extra} \tag{13}$$

Here, u_T is the control effort for torque tracking, u_f is the friction compensation control and u_{extra} is the extra torque compensation control. The unknown function $\tilde{f}(T_{extra}, T_f \mid \theta)$ is the estimated output of fuzzy logic for friction and extra torque.

3.1.1. Stability analysis

To prove stability of the closed loop, the Lyapunov function is chosen as

$$\begin{aligned} V &= \frac{1}{2}\left(s^2 + \sum_{i=1}^{n} \eta_i \tilde{\theta}^2{}_i\right) \\ \dot{V} &= s\dot{s} + \sum_{i=1}^{n} \eta_i \tilde{\theta}_i \dot{\tilde{\theta}}_i \end{aligned} \tag{14}$$

Here $\tilde{\theta}_i = \hat{\theta}_i - \theta_i$. Combine Eq. (11) and Eq. (14)

$$\dot{V} = s\left(\left(-a\dot{T}_L + bu - f\left(T_{extra}, T_f\right)\right) - \ddot{T}_n\right) + \sum_{i=1}^{n} \eta_i \tilde{\theta}_i \dot{\tilde{\theta}}_i \tag{15}$$

Define $\dot{T}_n = -\ddot{T}_r + \lambda \dot{e}$ and combine Eq. (12) into Eq. (15)

$$\begin{aligned} \dot{V} = s\Big(&-a\dot{T}_L + a\dot{T}_L + \hat{f}\left(T_{extra},\ T_f\right) \Big| \theta + \ddot{T}_n - K_d s - w.sgn(s) \\ &- f\left(T_{extra},\ T_f\right) - \ddot{T}_n\Big) + \sum_{i=1}^{n} \eta_i \theta_i \dot{\theta}_i \end{aligned} \tag{16}$$

The fuzzy approximation error is defined as [3]

$$\begin{aligned} e_f &= f\left(T_{extra}, T_f\right) - \tilde{f}\left(T_{extra}, T_f\right) | \theta^* \\ \theta_i \xi_i\left(\dot{\theta}\right) &= \hat{f}\left(T_{extra}, T_f\right) / \theta - \tilde{f}\left(T_{extra}, T_f\right) | \theta^* \end{aligned} \tag{17}$$

Combining Eq. (16) and Eq. (17) yields [16]

$$\dot{V} = s\left(\hat{f}\left(T_{extra},\ T_f\right) / \theta - f\left(T_{extra},\ T_f\right) - K_d s - w.sgn(s)\right) + \sum_{i=1}^{n} \eta_i \theta_i \dot{\theta}_i \tag{18}$$

$$\begin{aligned} \dot{V} = s\Big(&\hat{f}\left(T_{extra},\ T_f\right) \Big| \theta - \tilde{f}\left(T_{extra},\ T_f\right) \Big| \theta^* - \left(\left(f\left(T_{extra},\ T_f\right) - \tilde{f}\left(T_{extra},\ T_f\right) | \theta^*\right)\right) \\ &- K_d s - w.\mathrm{sgn}(s)\Big) + \sum_{i=1}^{n} \eta_i \theta_i \dot{\theta}_i \end{aligned} \tag{19}$$

Using Eq. (19) the following adaptive law is derived

$$\dot{\theta}_i = -\eta_i^{-1} s_i \xi_i\left(\theta,\ \dot{\theta}\right) \tag{20}$$

By replacing Eq. (20) in Eq. (19) and simplifying

$$\dot{V} = s\left(-e_f - K_d s - w.\mathrm{sgn}(s)\right) \tag{21}$$

It is assumed that ideally fuzzy compensating error e_f is approaching zero, and by choosing $K_d > 0$ it can be shown that

$$\dot{V} = -sK_d s \le 0 \tag{22}$$

http://dx.doi.org/10.5772/62710

3.1.2. Results and discussion

For simulations and validity of the proposed control scheme, the following parameters are used. Total inertia of the system is given as $J = 0.04Kg/m^2$, resistance $R = 7.5\Omega$, inductance $L = 1mH$, motor torque constant $k_t = 5.7325Nm/A$, back emf constant $k_b = 5.7325Nm/V$, viscous coefficient $B = 0.244Nm/rad/s$, torque sensor stiffness $K_s = 950Nm/rad$, static friction $f_s = 3Nm$, coulomb friction $f_c = 2.7Nm$, $\sigma_0 = 260Nm/rad$, $\sigma_1 = 2.5Nm - s/rad$, $\sigma_0 = 0.022Nm - s/rad$and Stribeck velocity $\alpha = 0.001rad/s$. The parameters of the controller are given as fuzzy learning rate $\eta_i = 0.0001$, amplifier gain $k_u = 10$, $k_d = 10$, $w = 1.5$, $\lambda = 15$.

3.1.3. Loading motor torque tracking performance

The testing of actuator is performed under the loading torque $T_r = 16\theta_a$ where "$C = 10$". From **Figure 3**, it is concluded that the output torque applied by the loading motor is exactly the same as the reference loading torque.

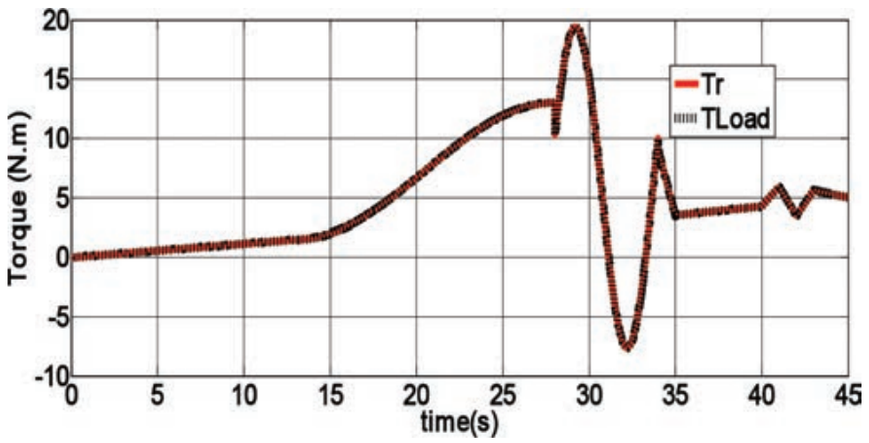

Figure 3. Loading motor closed loop performance.

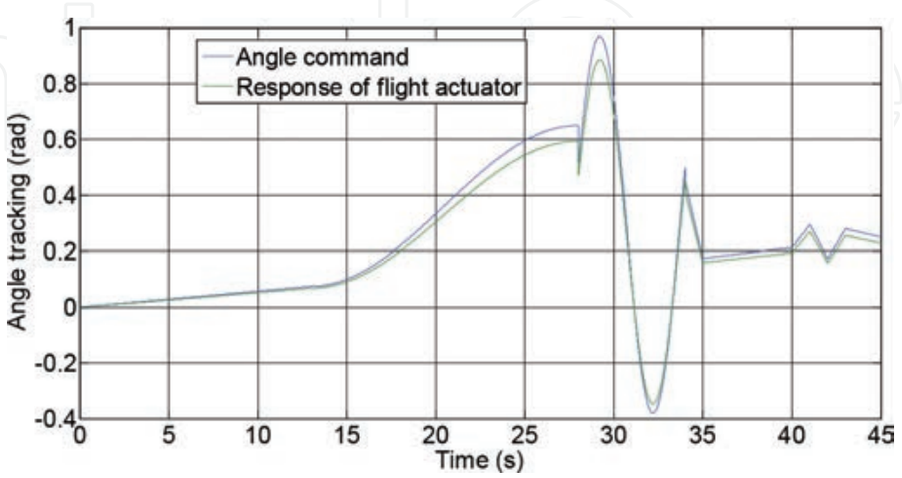

Figure 4. Flight actuator closed loop performance with aerodynamics load.

3.1.4. Flight actuator angle tracking performance under load

Figure 4 presents the testing results and the qualification of the autopilots of the flight actuators under the aerodynamic loading shown in **Figure 3**, which is mechanically transmitted from loading motor. From the results provided, it is concluded that the flight actuator under can withstand the non-linear profile of the aerodynamic load supplied. Moreover, the autopilot position controller is also robust and the position tracking errors are small enough.

4. Conclusion

This chapter covers the basic working principle of the load simulator system for testing of the flight actuators. As a case study, a real test data was used as reference command to the flight actuators and the load calculator unit. The output of the load calculator system provides the reference loading torque command for the loading motor, which is working in closed loop. From the results presented in this chapter, it is concluded that the proposed hardware setup is feasible to be utilized for cost-effective testing and qualification of the flight actuation system.

Author details

Nasim Ullah

Address all correspondence to: nasimullah@cusit.edu.pk

City University of Science and IT, Peshawar, Pakistan

References

[1] Zongxia J., Chenggong L., and Zhiting R.. The extraneous torque and compensation control on the electric load simulator. In: International Symposium on Instrumentation and Control Technology; 2003. pp. 723–727.

[2] Wang X., Wang S., and Yao B.. Adaptive robust control of linear electrical loading system with dynamic friction compensation. IEEE/ASME International Conference on Adavanced Intelligent Mechatronics, 2010: pp. 908–913.

[3] Nasimullah S. Wang, and Aslam J.. Adative robust control of electrical load simulator based on fuzzy logic compensation. International Conference on Fluid Power and Mechatronics, 2011: pp. 861–867.

[4] Wang X. and Wang S.. Electrical load simulator based on velocity-loop compensation and improved fuzzy-PID. IEEE International Symposium on Industrial, 2009: pp. 238–243.

[5] Chen K., Wang J., and Yan J.. Experiment and study of electric loading simulator for linear rudder. Electronic Engineering, 2008, 1: 4798–4802.

[6] Changhua L.. Design of electric loading system in flight simulator based on PIDNN [A]. International Conference on Mechatronic Science, Electric Engineering and Computer, 2011: pp. 2623–2626.

[7] Liu S., Wang M., Tian K., and Wang Y.. Research on loading simulation of DC torque motor for electrical load simulator. IEEE Conference on Industrial Electronics and Applications [C], 2008: pp. 1146–1150.

[8] Huang Y., Chen K., and .Wei J. Robust controller design and experiment for electric load simulator. International Advanced Computer Theory and Engineering, 2010: pp. 236–240.

[9] Truong D. Q., Kwan A. K., and Il Yoon J.. A study on force control of electric-hydraulic load simulator using an online tuning quantitative feedback theory [A]. International Conference on Control, Automation and Systems [C], 2008, pp. 2622–2662.

[10] Me H., Hong S., and Ik S.. Mechatronics Precise friction control for the nonlinear friction system using the friction state observer and sliding mode control with recurrent fuzzy neural networks [J]. Mechatronics, 2009, 19(6): 805–815.

[11] Erfanian V. and Kabganian M.. Adaptive trajectory control and friction compensation of a flexible-link robot [J]. Scientific Research and Essay, 2009, 4(4): 239–248.

[12] Angue-mintsa H. and Belleau C.. Adaptive Position Control of an Electrohydraulic Servo System With Load Disturbance Rejection and Friction Compensation [J]. Journal of Dyanmic systems, Measurment and Control, 2011, 133(6): 1–8.

[13] Lu L., Yao B., Wang Q., and Chen Z.. Adaptive robust control of linear motor systems with dynamic friction compensation using modified LuGre model [A]. International Conference on Advanced Intelligent Mechatronics [C], 2008: pp. 961–966.

[14] Messaoudi M., Sbita L., and Abdelkrim M. N.. A robust nonlinear observer for states and parameters estimation and on-line adaptation of rotor time constant in sensorless induction motor drives. International Journal of physical sciences, 2007, 2(8): 217–225.

[15] Ullah N. , Shaoping W., Khattak MI. and Shafi M.. Fractional order adaptive fuzzy sliding mode controller for a position servo system subjected to aerodynamic loading and nonlinearities [J]. Aerospace Science and Tehcnology, 2015, 43: 381–387.

[16] Ullah N., Han S., and Khattak MI.. Adaptive fuzzy fractional-order sliding mode controller for a class of dynamical systems with uncertainty. Transactions of the Institute of Measurement and Control, 2015, June 3, 20150142331215587042